Journal of Ceramic Processing Research. Vol. 17, No. 6, pp. 564~568 (2016)

J O U R N A L O F
Ceramic Processing Research

Effects of flow rate of hydrogen and substrate temperature on the characteristics of IZO thin films for OLEDs

K. H. Seo and K. M. Lee*

Dept. of Materials Engineering, Korea University of Technology and Education, Cheonan, Chungnam, 330-708, Korea

This study examined the effects of the H_2 flow rate and the substrate temperature on the structural, electrical, and optical characteristics of the IZO thin films intended for use as anode materials in OLEDs (organic light emitting diodes). These IZO thin films were deposited by RF magnetron sputtering at room temperature and 300 °C at various H_2 flow rates. To examine the effects of H_2, the H_2 flow rate in the argon mixing gas was changed from 0.1 sccm to 0.9 sccm. IZO thin films deposited at room temperature showed an amorphous structure, whereas IZO thin films deposited at 300 °C showed a crystalline structure with an (222) preferential orientation regardless of the H_2 flow rate. The electrical resistivity of the IZO thin films decreased with increasing H_2 flow rate under Ar+H_2. The change in the electrical resistivity with increasing H_2 flow rate was interpreted mainly in terms of the charge carrier concentration rather than the charge carrier mobility. The electrical resistivity of the amorphous-IZO films deposited at R.T. was lower than that of the crystalline-IZO thin films deposited at 300 °C. All the films showed an average transmittance of more than 83% in the visible range. The optical band gap of the IZO films increased with increasing H_2 flow rate. The current density and luminance of the OLED devices with IZO thin films deposited at room temperature in 0.9 sccm H_2 ambient gas were the highest among the films examined. These properties were attributed to the improved optical band gap, which plays a major role in the OLED device performance.

Key words: IZO thin film, RF magnetron sputtering, Flow rate of hydrogen gases, Substrate temperature, Optical band gap, OLED device.

Introduction

Transparent conducting oxide (TCO) thin films have been studied extensively for applications to display devices, such as liquid crystal displays (LCDs), plasma display panels (PDPs) and organic light emitting diodes (OLEDs) [1-3]. Of the TCO films, indium tin oxide (ITO) thin films have been used extensively in these devices because of their high transmittance in the visible range and low electrical resistivity [4, 5]. On the other hand, to have high electrical conductivity and high transmittance, ITO thin films must be deposited and annealed at temperatures higher than 250 °C and 300 °C, respectively. This high temperature post-annealing makes ITO films rough due to crystallization, which leads to significant deterioration of the device reliability [4, 5].

Recently, new transparent conducting oxides, such as IZO (indium zinc oxide) thin films have emerged as promising anode materials for OLEDs owing to their low deposition temperature, high work function, low resistivity, excellent chemical stability, and high transmittance over 80% in the visible spectrum [6-8]. IZO thin films can be deposited by RF magnetron sputtering, which has been used widely because of its advantageous features including simple apparatus, high deposition rates, and low deposition temperature. The properties of IZO thin films depend strongly on the stoichiometry, microstructure, and nature of the impurities, and it is obvious that deposition processes associated with different control parameters induce slightly different characteristics in thin films [6-8]. Several groups have examined the effects of ambient gas in reactive sputtering on the electrical and structural properties of TCO films [9-14]. Previously, our group has discussed the roles of the partial pressure of O_2 and H_2 on the structural, optical and electrical properties of RF magnetron sputtered TCO films [15-16]. From these studies, it was concluded that the electrical resistivity correlates strongly with the stoichiometry of the IZO thin films. Therefore, it is interesting to study the effect of the ambient gas on the structure and electrical resistivity, especially on the charge carrier concentration and charge carrier mobility of IZO thin films. This study examined the effects of the substrate temperature on the structural, electrical, and optical characteristics of IZO thin films on the performance of OLED devices. For this purpose, Zn-doped In_2O_3 (IZO) films were deposited by RF magnetron sputtering at room temperature and 300 °C at various H_2 flow rates. The electrical resistivity and optical band gap of the IZO thin films were examined systematically. To determine the effect of the electrical resistivity and/or the optical band gap on the performance of OLED devices, organic materials and

*Corresponding author:
Tel : +82-41-560-1320
Fax: +82-41-560-1360
E-mail: kmlee@koreatech.ac.kr

Table 1. Conditions of sputtering IZO thin films.

Deposition parameters	Conditions
Target	In_2O_3/ZnO (90/10 wt.%)
Substrate	Glass (corning 7059)
Initial pressure	5.0×10^{-6} torr
Working pressure	6.0×10^{-3} torr
Film thickness	200 nm
Substrate temperature	Room temp. and 300 ºC
RF power	100 W
Gas ambient	Ar:40, H_2 flow rate:0.1-0.9 sccm

cathode electrode were deposited sequentially on the IZO thin films. The electrical characteristics of the OLED devices, such as current density vs. voltage and luminescence vs. voltage, were measured.

Experimental

IZO thin films were deposited by RF magnetron sputtering from a target containing 90% indium oxide and 10% zinc oxide. The glass substrates (Corning 7059, Samsung Corning Precision Glass, Korea) were first cleaned and rinsed in deionized water. The sputtering chamber was evacuated using a turbomolecular pump to the base pressure of about 1.0×10^{-6} torr. To examine the influences of H_2, the H_2 flow rate in the argon mixing gas was changed from 0.1 sccm to 0.9 sccm. The substrate temperature was either room temperature or 300 ºC. Table 1 lists the experimental conditions for the deposition of IZO thin films.

The microstructural observations and crystal orientation of the IZO thin films were evaluated by X-ray diffraction (XRD, Rigaku, RTP300RC) and field emission scanning electron microscopy (FE-SEM, JEOL, JSM7500F), respectively. The optical transmittance of the IZO thin films was measured using an ultraviolet spectrophotometer (model cary500, Varian, Korea). The film thickness was determined using a surface profile measurement system and the electrical properties of the IZO thin films were measured using Hall Effect measurements (model HMS-3000, Ecopia, Korea). The organic materials and cathode electrode were deposited sequentially on the TCO thin films to give a device structure of IZO/α-NPD(N,N-Di(naphthalene-1-yl)-N,N-diphenyl-benzidine)/DPVB ((diphenylvinyl) benzene)/Alq_3/LiF/Al. DPVB was used as a blue emitting material. The electrical characteristics, such as current density vs. voltage and luminescence vs. voltage of the OLED devices, were evaluated using a spectrometer (CS-1000A, Konika Minolta Sensing INT, Japan).

Results and Discussion

XRD patterns of the IZO thin films deposited by RF magnetron sputtering sputtering are presented in Fig. 1. The figure clearly shows that the IZO thin films deposited at room temperature were amorphous, whereas the thin films deposited at 300 ºC showed a sharp (222) peak at 30.54 º 2θ, indicating that the IZO film has a (111) preferential orientation. Furthermore, with increasing hydrogen concentration, the intensity of

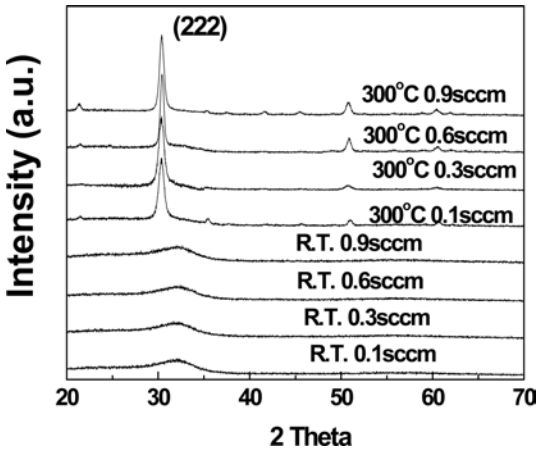

Fig. 1. XRD patterns of IZO thin films deposited at (a) room temperature and (b) 300 ºC with various H_2 flow rate.

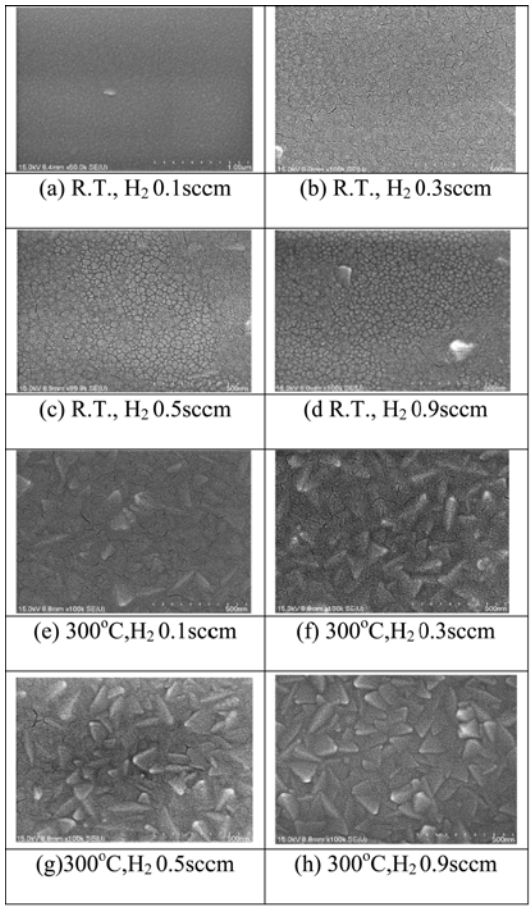

Fig. 2. Field effect scanning electron microscope images of IZO thin films with different deposition temperature and various H_2 flow rate.

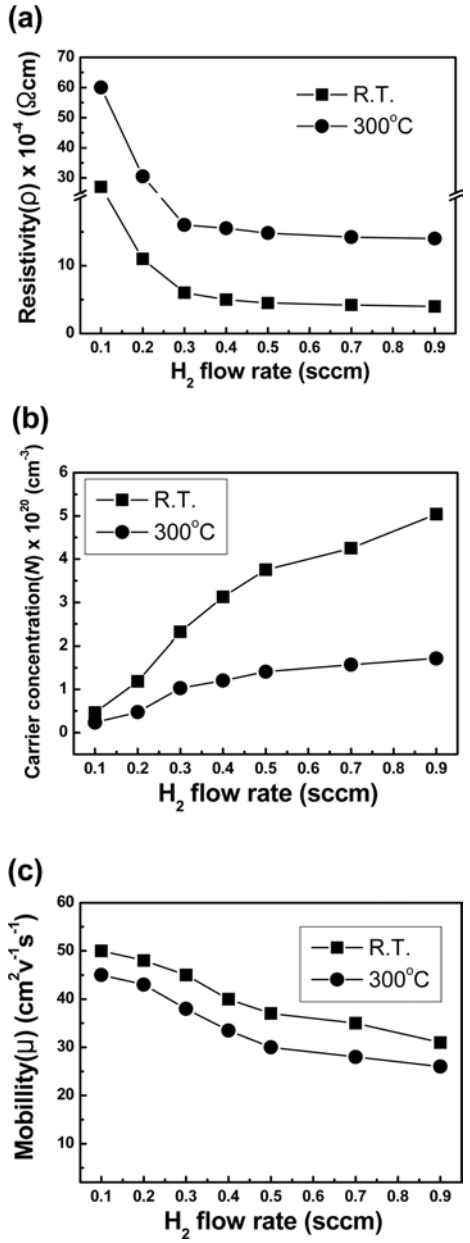

Fig. 3. (a) Resistivity(ρ), (b) charge carrier concentration(*N*), and (c) charge carrier mobility (i) of IZO thin films with different deposition temperature and various H_2 flow rate.

the (222) peak remained unaltered. A specific preferred orientation of the thin film can be discussed based on the strain and surface energies [17]. At thin film thicknesses, the surface energy controls growth, whereas at thick film thicknesses the strain energy predominates. Based on the above discussions, the (111) plane of IZO thin films has the lowest strain.

Because the surface properties of the TCO thin films for anode materials can affect the characteristics of OLED devices [18], it is important to examine the surface morphology of the IZO thin films. Fig. 2 shows the microstructural features of the IZO thin films with different H_2 flow rates and substrate temperature. As shown in the figures, secondary phases were not observed.

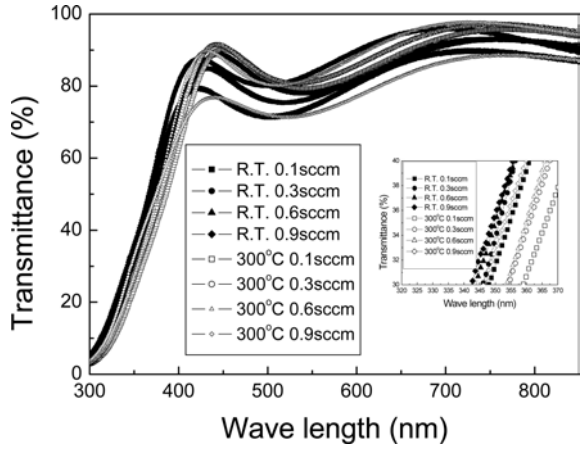

Fig. 4. Optical transmittance spectra of IZO thin films with different deposition temperature and various H_2 flow rate.

The grain sizes in the IZO thin films were similar regardless of the H_2 flow rate and substrate temperature. On the other hand, with increasing H_2 concentration, small cracks were observed between the grains, and the amount of hazy phases decreases (Fig. 2), which suggests that the film surface could be etched off by hydrogen bombardment through a physical interaction [19]. From Figs. 1 and 2, it appears that the flow rate of hydrogen gases and substrate temperature have an important effect on the physical characteristics, such as the crystal orientation and microstructure of the thin films.

Fig. 3 shows the electrical resistivity (ρ), charge mobility (μ), and charge carrier concentration (*N*) of the IZO thin films with different deposition temperatures and various H_2 flow rates. As shown in the figures, the electrical resistivity decreases very sharply in an Ar+H_2 atmosphere and is nearly the same, regardless of the H_2 flow rate. This can be interpreted in terms of the drastic increase in the charge carrier concentration. The results of Fig. 3 reveal the importance of keeping in mind that the electrical resistivity of IZO thin films is mainly associated with the charge carrier concentration rather than the charge carrier mobility. It is now well established that oxygen vacancies in In_2O_3-based TCO thin films act as donors, and their presence make the film less resistive [20]. During reactive sputtering in ambient hydrogen, due to the reducing property of hydrogen, oxygen vacancies are created in IZO thin films. Therefore, the resistivity of such films deposited in an Ar+H_2 ambient environment decreases. Furthermore, the figures clearly show that the electrical resistivity of the amorphous-IZO films deposited at R.T. was lower than that of the crystalline-IZO thin films deposited at 300 ºC, which can be interpreted mainly in terms of the charge carrier mobility rather than the charge carrier concentration.

Fig. 4 shows the optical properties of the IZO films with different deposition temperatures and various H_2 flow rates. The figure shows that the mean transmittance in the visible wavelength region was more than 83% for all IZO thin films. As the inset in Fig. 4 clearly shows, the

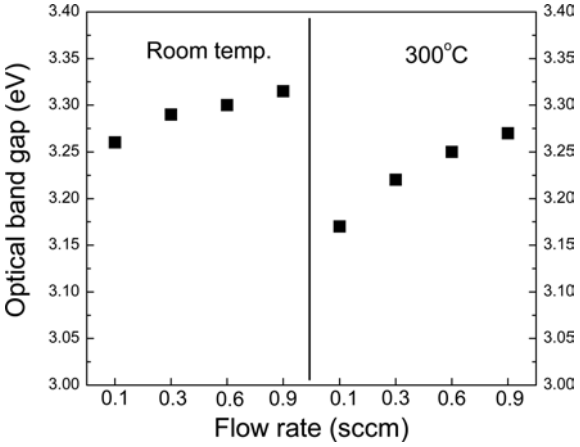

Fig. 5. Optical band gap of IZO thin films as a function of the flow rate of H_2 and the substrate temperature.

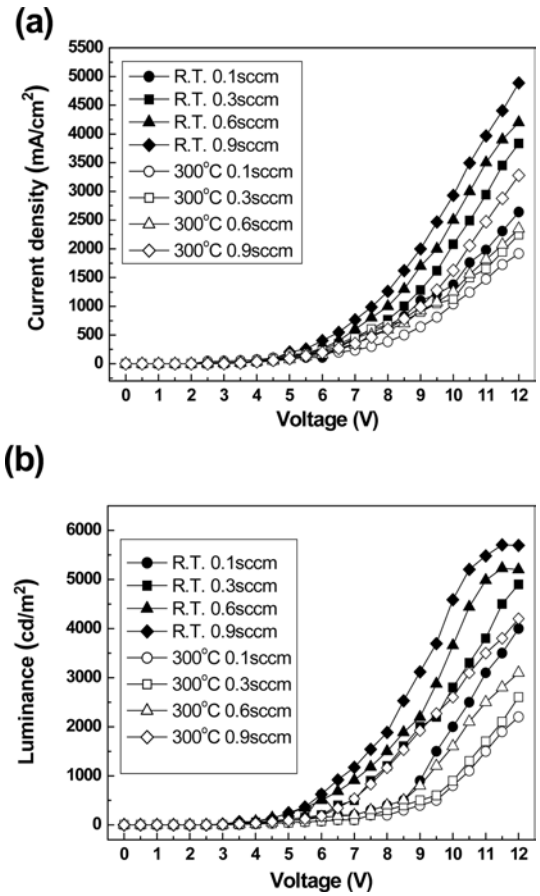

Fig. 6. (a) I-V and (b) L-V characteristics of OLED devices.

UV absorption edge was shifted by a small wavelength with increasing H_2 flow rate and substrate temperature, indicating broadening of the optical band gap.

The absorption coefficient, α, can be expressed by the equation, $\alpha = (1/d)\ln(1/T)$, where T is the transmittance and d is the thin film thickness (200 nm in our experiment). The optical band gap (E_{opt}) of the IZO thin films can be determined from the experimental spectra of the absorption coefficient (α) as a function of the photon energy (hυ) using the following equation [21]:

$$(\alpha h\upsilon)^2 = C(h\upsilon - E_{opt}) \quad (1)$$

where C is a constant for a direct transition, h is Planck's constant, and υ is the frequency of the incident photon.

$(\alpha h\upsilon)^2$ was plotted as a function of the photon energy (hυ) to estimate the band gap of the IZO thin films. Fig. 5 shows the optical band gap of the IZO films, as determined from the obtained transmittance spectra. As shown in the figure, the optical band gap of the IZO films increased with increasing H_2 flow rate. Furthermore, the optical band gap of the IZO films deposited at 300 °C was lower than that of the film deposited at room temperature at the same hydrogen flow rate. An increase in the Fermi level in the conduction band of a degenerate semiconductor leads to band gap widening, which is consistent with the present experimental results [20, 22-23]. °C

Fig. 6 shows the characteristics of the current density vs. voltage and the luminance vs. voltage of the OLED devices with the IZO thin film deposited in various ambient gases for comparison. The device structure was IZO/α-NPD/DPVB/Alq_3/LiF/Al. DPVB was used as a blue emitting material. As shown in Fig. 6, the current density and luminance of the OLED devices were observed in the following order: $H_{R.T.\ 0.9\ sccm} > H_{R.T.\ 0.6\ sccm} > H_{R.T.\ 0.3\ sccm} > H_{300\ ℃\ 0.9\ sccm} > H_{R.T.\ 0.1\ sccm} > H_{300\ ℃\ 0.6\ sccm} > H_{300\ ℃\ 0.3\ sccm} > H_{300\ ℃\ 0.1\ sccm}$. This order was consistent with that of the optical band gap energies of the IZO films with different deposition temperature and various H_2 flow rates (as shown in Fig. 5). If the electrical resistivity is treated as the main parameter affecting the current density and the luminance, the current density and the luminance of OLED devices deposited in a H_2 atmosphere should be nearly the same above 0.5 sccm H_2. Therefore, the results of Fig. 6 clearly show that hole injecting ability of the IZO anode is largely dependent on the optical band gap of IZO thin films. As shown in Figure 6, the current density and the luminance of the OLED devices with IZO thin films deposited at room temperature in 0.9sccm H_2 were the highest among the films considered. Figes 5 and 6 show that the optical band gap of IZO thin films plays a major role in OLED device performance, particularly the current density and luminance.

Conclusions

The structural, electrical and optical properties of the IZO thin films were examined systematically for use as the anode contact in OLED devices. IZO thin films were deposited by RF magnetron sputtering at room temperature and 300 °C at various H_2 flow rates. The IZO thin films deposited at room temperature showed an amorphous structure, whereas the IZO thin films deposited at 300 °C showed a crystalline structure with

a (222) preferential orientation regardless of the H_2 flow rate. The electrical resistivity decreases very sharply in an $Ar+H_2$ atmosphere and is nearly the same, regardless of the H_2 flow rate. The change in the electrical resistivity with increasing H_2 flow rate was interpreted mainly in terms of the charge carrier concentration rather than the charge carrier mobility. The electrical resistivity of the amorphous-IZO films deposited at R.T. was lower than that of the crystalline-IZO thin films deposited at 300 °C. The change in the electrical resistivity with increasing substrate temperature was interpreted mainly in terms of the charge carrier mobility rather than the charge carrier concentration. All the films showed a mean transmittance greater than 83% in the visible range. The optical band gap of the IZO films increased with increasing H_2 flow rate. Furthermore, the optical band gap of the IZO films deposited at 300 °C was lower than that of the film deposited at room temperature at the same H_2 flow rate. The current density and luminance of the OLED devices with IZO thin films deposited at room temperature in 0.9 sccm H_2 ambient gas were the highest among the films examined. These properties were attributed to the improved optical band gap, which plays a major role in the performance of OLED devices.

References

1. K. Ishibashi, K. Hirata, and N. Hosokawa, Journal of Vacuum Science & Technology A. 10 (1992) 1718-1722.
2. K. Tominaga, T. Ueda, T. Ao, M. Kataoka, and I. Mori, Thin Solid Films 281-282 (1996) 194-197.
3. Y. Hoshi, H. Kato, and K. Funatsu, Thin Solid Films 445 (2003) 245-250.
4. N. Taga, M. Maekawa, Y. Shigesato, I. Yasui, M. Kamei, and T. E. Haynes, Jpn. J. Appl.Phys. 37 (1998) 6524-6529.
5. C. Nunes de Carvalho, A. M. Botelho do Rego, A. Amaral, P. Brogueira, and G. Lavareda, Surface and Coatings Technology 124 (2000) 70-75.
6. Y.S. Jung, J.Y. Seo, D.K. Lee, and D.Y. Jeon, Thin Solid Films 445 (2003) 63-71.
7. K.H. Noh, M.K. Choi, S.H. Park, and H.R, Joo, Hankook Kwanghan Hoeji 13 (2002) 455-459.
8. D.C. Paine, B. Yaglioglu, Z. Beiley, and S. Lee, Thin Solid Films 516 (2008) 5894-5898.
9. Y.S. Rim, H.J. Kim, and K.H. kim, Thin Solid Films 518 (2010) 6223-6227.
10. C.E. Kim, H.S. Shin, P. Moon, H.J. Kim, and I. Yun, Current Applied Physics 9 (2009) 1407-1410.
11. C.G. Choi, K. No, W.J. Lee, H.K. Kim, S.O. Jung, W.J. Lee, W.S. Kim, S.J. Kim, and C. Yoon, Thin Solid Films 258 (1995) 274-278.
12. R. Das, K. Adhikary, and S. Ray, Appl. Surf. Sci. 253 (2007) 6068-6073.
13. J.Y. Kim, D.M. Lee, J.K. Kim, S.H. Yang, J. M. Lee, Appl. Surf. Sci. 265 (2013) 145-148.
14. A. Singh, S. Chaudhary, D. K. Pandya, Acta Mater. 77 (2014) 125-132.
15. S.H. Han, D.B. Jo, K.M. Lee, Electron. Mater. Lett. 9 (2013) 43-48
16. Y.L. Lee, K.M. Lee, Trans. Electr. Electron. Mater. 10 (2009) 203-207.
17. S.I. Jun, T.E. Mcknight, M.L. Simpson, P.D. Rack, Thin Solid Films 476 (2005) 59-64.
18. D. Xu, Z. Deng, Y. Xu, J. Xiao, C. Liang, Z. Pei, C. Sun, Phys. Lett. A 346 (2005) 148-152.
19. L. Raniero, I. Ferreira, A. Pimentel, A. Goncalves, P. Canhola, E. Fortunato, R. Martins, Thin Solid Films 511-512 (2006) 295-298.
20. J. Jia, A. Takasaki, N. Oka, Y. Shigesato, J. Appl. Phys. 112 (2112) 013718.
21. J. Tauc, R. Grigorovichi, A. Vancu, Phys. Stat. Sol. 15 (1966) 627-637.
22. J.J. Ortegaa, M.A. Aguilar-Frutis, G. Alarcón, C. Falcony, V.H. Méndez-García, J.J. Araiza, Mater. Sci. Eng. B 187 (2014) 83-88.
23. D.H. Oh, Y.S. No, S.Y. Kim, W.J. Cho, J.Y. Kim, and T.W. Kim, J. Ceram. Proc. Res. 12 (2011) 488-491.